Portable Ultrafast Blue Light Sources Designed With Frequency Doubling in KTP and $KNbO_3$

Ben Agate, Edik U. Rafailov, *Member, IEEE*, Wilson Sibbett, Solomon M. Saltiel, Kaloian Koynov, Mikael Tiihonen, Shunhua Wang, Fredrik Laurell, Philip Battle, Tim Fry, Tony Roberts, and Elizabeth Noonan

***Abstract*—We demonstrate an effective means of achieving compact, truly portable, and entirely self-contained ultrafast blue light sources. Using a variety of nonlinear media to achieve simple second-harmonic generation of a femtosecond Cr:LiSAF laser, we investigate the relative merits of aperiodically poled bulk and waveguide nonlinear crystals in comparison to periodically poled structures. Such a compact and convenient source of ultrashort laser pulses in the blue spectral region could be of great interest for on-site applications spanning a host of disciplines, such as biomedical imaging, optical micromanipulation, and high-resolution spectroscopy.**

***Index Terms*—Diode-pumped lasers, frequency conversion, mode-locked lasers, periodic structures, waveguides.**

I. Introduction

THE RECENT enthusiasm for research in photobiology, such as microscopy, optical micromanipulation, and biomedical imaging, continues to justify the need for compact low-cost lasers that demonstrate true portability and practicality. The development and exploitation of photonics-based techniques that are applicable to biology and medicine is of particular interest. Laser sources at the shorter blue and ultraviolet wavelengths provide clear advantages over infrared lasers in allowing for stronger beam focusing, enhanced resolution in multidimensional imaging techniques [1] and high-resolution spectroscopy [2]. By using ultrashort-pulse lasers in preference to continuous-wave sources, it is possible to investigate ultrafast biological processes [3], increase the resolution of microscopy [4], [5], and amplify subtle signals in nonlinear and multiphoton techniques [6]–[8]. Femtosecond pulses in the blue spectral region have already been utilized in the study of protein dynamics [9].

Manuscript received April 19, 2004; revised September 1, 2004. This work was supported in part by the United Kingdom Engineering and Physical Sciences Research Council.

B. Agate is with the Interdisciplinary Centre for Medical Photonics, School of Physics and Astronomy, University of St. Andrews, St. Andrews KY16 9SS, U.K. (e-mail: mba@st-andrews.ac.uk).

E. U. Rafailov and W. Sibbett are with the J. F. Allen Physics Research Laboratories, School of Physics and Astronomy, University of St. Andrews, St. Andrews KY16 9SS, U.K. (e-mail: er8@st-andrews.ac.uk).

S. M. Saltiel is with the Faculty of Physics, University of Sofia, BG-1164 Sofia, Bulgaria (e-mail: saltiel@phys.uni-sofia.bg).

K. Koynov is with the Max Planck Institute for Polymer Research, D-55128 Mainz, Germany (e-mail: koynov@mpip-mainz.mpg).

M. Tiihonen, S. Wang, and F. Laurell are with the Department of Physics, Royal Institute of Technology, SE-10691 Stockholm, Sweden.

P. Battle, T. Fry, T. Roberts, and E. Noonan are with AdvR, Inc., Bozemon, MT 59718 USA.

Digital Object Identifier 10.1109/JSTQE.2004.837714

Straightforward frequency doubling of near-infrared femtosecond lasers remains one of the simplest and most efficient access routes into the blue spectral region, due mainly to the inherently high-peak intensities of the ultrashort laser pulses. While conventional titanium–sapphire lasers have long been the market leader in providing femtosecond pulses in the near-infrared, their impractical size, cost, and power requirements render such sources impractical for space-limited on-site applications in biomedical and clinical laboratories. Consequently, we have recently demonstrated how small-scale femtosecond Cr:LiSAF lasers have much to offer in combining superior operational efficiencies with impressive design flexibility [10].

In this paper, we describe how this compact Cr:LiSAF laser design can be used to demonstrate an attractively simple approach to developing a number of portable ultrafast blue light sources. With a femtosecond Cr:LiSAF laser operating at around 850 nm, we access the blue spectral region with a series of investigations into second-harmonic generation (SHG) using four different SHG crystals. The performance of aperiodically poled potassium titanyl phosphate (appKTP) in bulk and waveguide form is compared to that of bulk potassium niobate $(KNbO_3)$ [11] and the periodically poled KTP (ppKTP) waveguide [12]. Each SHG crystal is placed in a very simple extra-cavity single-pass arrangement at room temperature, requiring minimal wavelength and temperature stabilization. The ultrashort-pulse blue light generated from all four SHG crystals is either femtosecond or picosecond in duration.

This investigation provides the means to compare and contrast the relative merits of bulk and waveguide nonlinear materials, as well as periodically and aperiodically poled structures. Observations show that while superior infrared-to-blue SHG efficiencies are achieved with bulk $KNbO_3$ and the ppKTP waveguide, aperiodically poled structures permit higher blue peak powers, shorter blue pulses, and broader tunability in the blue spectral region. To support our experimental findings, we provide complementary modeling on the performance of the bulk and waveguide SHG crystals.

II. Portable Femtosecond Infrared Laser

The portable ultrafast blue light sources described here take advantage of a previously reported ultra-compact femtosecond Cr:LiSAF laser design [10], [13]–[15]. The extremely low pump-threshold conditions (∼22 mW to sustain modelocking) associated with this Cr:LiSAF laser permit the use of inexpensive (∼$40 U.S.) single-narrow-stripe AlGaInP red laser diodes (50–60 mW) as a pump source [16]. Their modest electrical drive requirements (∼100 mA current, ∼200 mW electrical

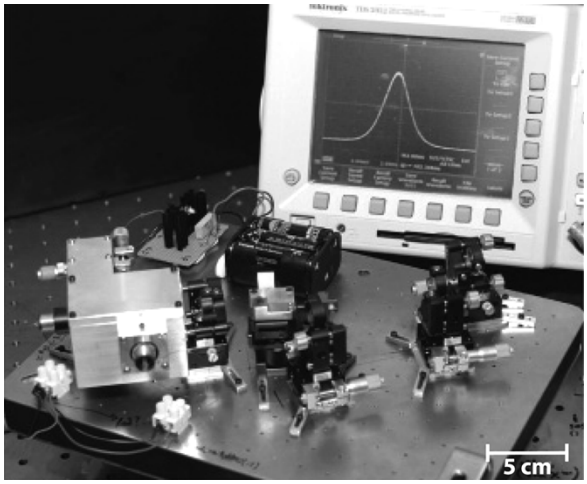

Fig. 1. Photograph of ultra-compact portable femtosecond infrared laser pumped by two inexpensive (∼$40 U.S.) single-narrow-stripe AlGaInP diodes and powered by standard penlight (AA) batteries [10]. Oscilloscope in the background records an intensity autocorrelation of the femtosecond pulses.

power) mean that these diodes require no active electrical cooling and can easily be powered for a number of hours by regular 1.5-V penlight (AA) batteries. With a maximum pump power from two pairs of pump laser diodes of ∼200 mW, the Cr:LiSAF laser crystal does not require any cooling. As a result, relatively inexpensive femtosecond Cr:LiSAF lasers with optical output powers up to 45 mW, robustly modelocked with a semiconductor saturable absorber mirror (SESAM), are achievable from entirely self-contained and portable units with dimensions of 22 × 28 cm. (A version of this laser design incorporating one pair of pump laser diodes is shown in Fig. 1.) A second pair of pump laser diodes can easily be incorporated onto the baseplate to maximize operational performance (Fig. 3).

The modest electrical drive requirements of these diodes, and the resulting option to power the laser with standard penlight (AA) batteries, allow these Cr:LiSAF lasers to boast an impressive electrical-to-optical efficiency of over 4%, which until recently [17] was the highest reported overall system efficiency of any femtosecond laser source. The amplitude stability of the laser output was observed to be very stable with a measured fluctuation of less than 1% for periods in excess of 1 h. These measurements were made on a laser that was not enclosed and located in a lab that was not temperature controlled. In a more enclosed and controlled local environment we would expect the amplitude fluctuations of this laser to be extremely small.

While the output powers achievable from these lasers is limited by the available power from the AlGaInP red laser diodes, there are already strong indications that commercial access to higher power diode lasers is imminent.

III. Simplified Blue Generation Scheme

By incorporating a straightforward but highly efficient frequency-doubling scheme into the compact femtosecond infrared laser of Fig. 1, a portable ultrafast blue light source can be achieved. To generate blue light (∼425 nm), all that is required is a single extracavity lens to focus the ∼850-nm

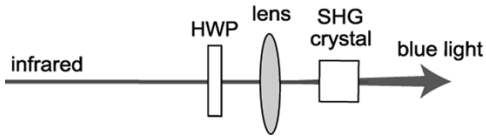

Fig. 2. Simplified efficient blue generation scheme. Single pass of pulsed infrared light through an extracavity lens and SHG crystal is all that is required. HWP may also be included if necessary.

light from a Cr:LiSAF laser through an SHG crystal in a single pass (Fig. 2). A half-wave plate (HWP) may also be required to select the appropriate linear polarization.

The phasematching conditions of all four SHG crystals investigated in this paper comfortably allow efficient and optimal blue-light generation at room temperature. In addition, the phasematching acceptance bandwidths (which define the accuracy to which the crucial parameters of SHG crystal temperature, fundamental wavelength, and incident angle must be maintained to successfully optimize the SHG process) are sufficiently relaxed to require minimal attention once the process has been optimized. Each SHG crystal is mounted on a basic thermoelectric cooler (TEC) which provides some current-controlled temperature stabilization should it be required.

IV. Experimental Performance of SHG Crystals

Investigations into the relative performance of the four SHG crystals were carried out using the femtosecond Cr:LiSAF laser illustrated in Fig. 3. Although this laser configuration differs slightly from the laser configuration of Fig. 1 (with an extra pair of pump laser diodes for increased output power [10] and an intracavity prism to allow wavelength tuning), these modifications do not compromise the small scale or potential portability of the laser construction.

With four single-narrow-stripe (SNS) pump laser diodes (two providing up to 60 mW at 685 nm, and two providing up to 50 mW at 660 nm), the laser was capable of generating 120–200-fs pulses at a repetition rate of 330 MHz and average output powers up to 45 mW. By simply tilting the angle of the output coupler, selection of the central operating wavelength was also possible between 825 and 875 nm (defined by the reflectivity bandwidth of the SESAM mirror). The infrared output beam was strongly linearly polarized (due to the Brewster surfaces of the Cr:LiSAF laser crystal) and the beam quality was measured to have an $M^2 = 1.1$. The stability of the pulsed output over a number of hours was observed to be excellent, together with negligible power degradation.

Each SHG crystal was assessed in an extracavity single-pass arrangement at room temperature (Fig. 3). An HWP was required for certain SHG crystals to provide the correct linear polarization. The relative performance of the four SHG crystals is summarized as follows.

A. Bulk $KNbO_3$

Bulk potassium niobate $(KNbO_3)$ is well suited to our needs because birefringent type-I noncritical phasematching (NCPM) can be exploited for highly efficient SHG of ∼850 nm at room temperature [11], [18], [19]. This NCPM avoids any spatial walkoff between the fundamental and second-harmonic (SH)

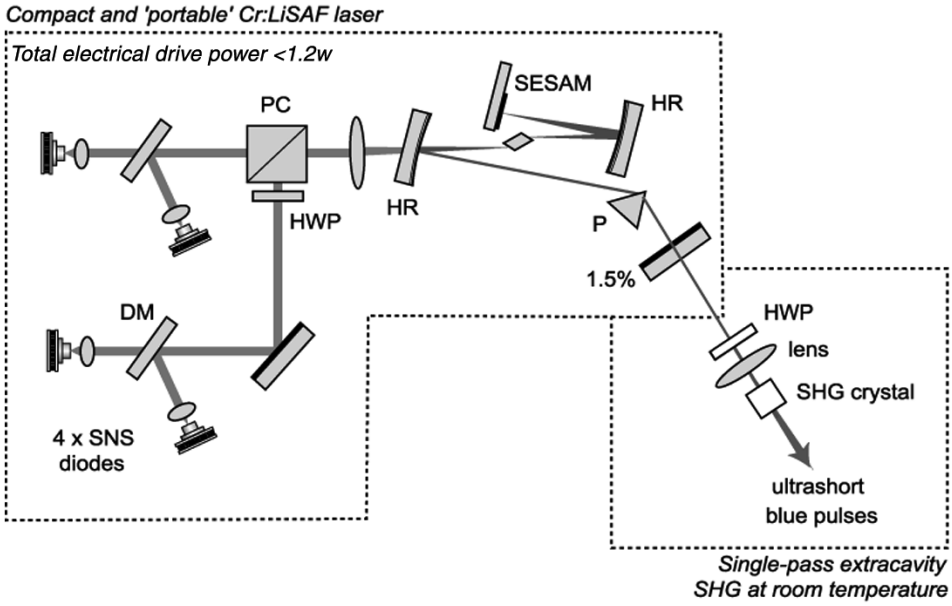

Fig. 3. Laser configuration for a compact ultrafast blue light source, incorporating four single-narrow-stripe (SNS) red laser diodes and an intracavity prism (P) for wavelength tuning (DM: dichroic mirror; HWP: half-wave plate; PC: polarization cube; HR: high reflector; 1.5%: output coupler). Entire system would fit onto a 22 × 28 cm baseplate.

beams, as well as maximizing the angular acceptance of the phasematching process.

Using an experimentally optimized focusing lens ($f = 15$ mm; spot radius, $w = 4.3$ μm) and a 3-mm $KNbO_3$ crystal (cut for NCPM at 22°C and 858-nm antireflective (AR) coated), up to 11.8 mW of blue average power with a spectral width up to $\Delta\lambda_{\rm SH} = 1.4$nm at 429 nm was generated with only 44.6 mW of incident fundamental. The maximum observed SHG conversion efficiency was as high as 30%. The overall efficiency of the electrical-to-blue process was over 1%, and the blue pulses were measured by autocorrelation to be ∼500 fs in duration [11].

The measured full-width at half-maximum (FWHM) wavelength and temperature acceptance bandwidths were 2.7 nm and 5°C, respectively. The beam quality parameter of the generated femtosecond blue beam was observed to be $M^2 = 1.8$. We believe the quality of the blue beam deteriorated slightly from the fundamental beam ($M^2 = 1.1$) as a result of the strong focusing. Because exact phasematching conditions are satisfied only at the beam centre, peripheral rays propagate under conditions of slight mismatch and as such accumulate phase distortions.

B. Waveguide ppKTP

Potassium titanyl phosphate (KTP) is another suitable nonlinear crystal for SHG, given that it can be waveguided and periodically poled to readily satisfy quasi-phasematching (QPM) conditions at room temperature. This waveguide ppKTP crystal, fabricated by ion exchange and periodically poled for SHG of ∼850 nm, had cross-sectional dimensions of ∼4 × 4 μm and was 11 mm in length (including a 3-mm Bragg grating section [20] which did not affect the performance of the Cr:LiSAF pump laser) and was not AR-coated.

With an appropriate aspheric lens ($f = 6.2$ mm) to optimize the coupling of the fundamental light into the waveguide, up to 5.6 mW of average output blue power with a spectral width of $\Delta\lambda_{\rm SH} = 0.6$ nm at 424 nm was achieved for 27 mW of incident fundamental. Accounting for a coupling efficiency of 70%, the associated internal SHG conversion efficiency within the waveguide was calculated to be as high as 37% [12]. With the Cr:LiSAF laser requiring no more than 1.2 W of electrical drive, this corresponds to an overall electrical-to-blue system efficiency of 0.5%. Evidence of a saturation and subsequent decrease in overall efficiency of the SHG process (Fig. 10) has been attributed to two-photon absorption of the SH wave [12]. The superiority of the ppKTP waveguide at low pulse energies is evident when comparing the slope efficiency per unit length of this experimental data (6.9% pJ^{-1} cm^{-1}) with other similar SHG experiments using bulk $KNbO_3$ (1.0% pJ^{-1} cm^{-1} [18],0.73% pJ^{-1} cm^{-1} [11]) and waveguide ppKTP (0.15% pJ^{-1} cm^{-1} [21]).

A broad temperature acceptance bandwidth of ΔT ∼30 °C (FWHM) centered at 18 °C easily permitted room-temperature operation. The characterization of fundamental pulses entering ($\Delta\tau \sim 170$ fs; $\Delta\nu\Delta\tau \sim 0.32$) and leaving ($\Delta\tau \sim 195$ fs; $\Delta\nu\Delta\tau \sim 0.37$) illustrated that these pulses were dispersed only slightly on propagation through the waveguide.

C. Bulk appKTP

While periodically poled materials are typically characterized by very narrow spectral acceptance bandwidths (<1 nm), aperiodically poled structures (characterized by a linear gradient in grating period) have the advantage of providing sufficiently broad spectral acceptance bandwidths to utilize more of the spectrum associated with picosecond [22] and femtosecond [23] pulses. They can also simultaneously provide some pulse compression of sufficiently prechirped incident pulses [24], [25].

The bulk appKTP crystal was flux-grown, 4 mm in length, and was not AR-coated. The grating periods varied from 4.1 to 4.3 μm in order to provide a fundamental bandwidth of

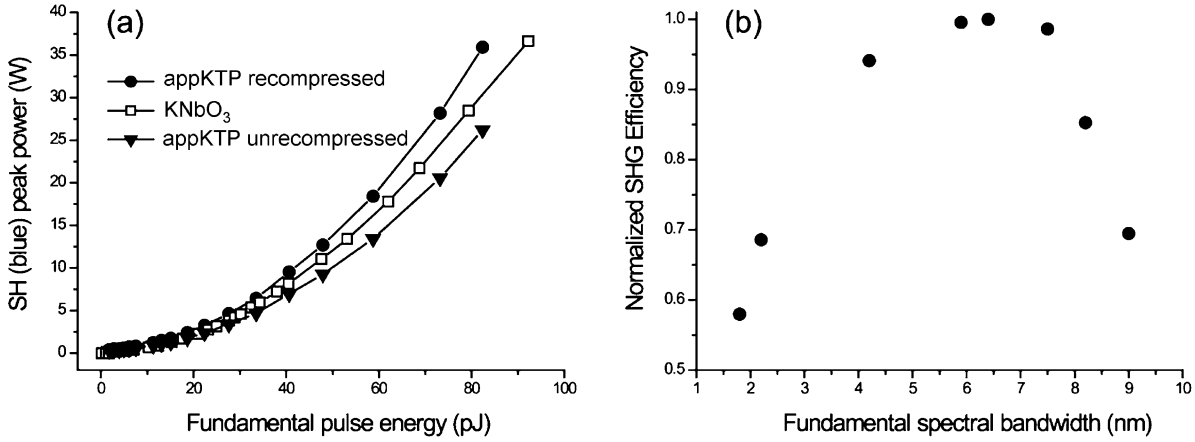

Fig. 4. (a) Relative blue pulse peak powers from bulk appKTP and bulk $KNbO_3$ crystals. (b) Dependence of SHG efficiency on fundamental spectral bandwidth of femtosecond Cr:LiSAF laser.

7 nm, for SHG at room temperature centered at 851 nm. With an experimentally optimized focusing lens ($f = 15$ mm, $w = 4.3$ μm), 3.2 mW of blue average power was produced at 429 nm with $\Delta\lambda_{\rm SH}$ up to 1.4 nm, from 27 mW of incident fundamental. This corresponds to an SHG conversion efficiency of 11.8% and an overall electrical-to-optical system efficiency of 0.3%. The wavelength acceptance bandwidth was measured to be 4.5 nm. In attempting to measure the temperature acceptance bandwidth, a negligible deterioration in SHG efficiency was observed when adjusting the bulk appKTP crystal temperature between 10°C and 50°C.

Although the absolute efficiency of the SHG process is lower than that achieved from the $KNbO_3$ crystal, Fig. 4(a) illustrates that either with suitable prechirping of the fundamental pulses or recompression of the generated blue pulses, the bulk appKTP crystal is able to provide ultrashort blue pulses with higher peak powers, P_{pk} ($P_{pk} = E_p/\Delta\tau_{SH}$, E_p is the pulse energy and $\Delta\tau_{\rm SH}$ is the SH pulse duration). Insufficient power was available to measure $\Delta\tau_{\rm SH}$ from the bulk appKTP crystal, but $\Delta\tau_{\rm SH}$ for our experimental conditions was calculated to be ~370 fs, shortening to a possible ~270 fs with suitable compression. The data for the $KNbO_3$ crystal in Fig. 4(a) was calculated using measured values of $\Delta\tau = 540$ fs and $\Delta\nu\Delta\tau = 0.39$ [11].

The bulk appKTP crystal is the least impressive of the four SHG crystals in terms of absolute SHG efficiency (Fig. 10). While the nonlinear coefficient $d_{\rm eff}$ of KTP (7.8 $\rm pmV^{-1}$) is less than that of $KNbO_3$ (12.5 $\rm pmV^{-1}$), an additional explanation is evident from Fig. 4(b), which is measured for constant fundamental pulse energy. This clear dependence of SHG efficiency on fundamental spectral bandwidth (broadened by the insertion of more glass from the intracavity prism in Fig. 3) is surprising, given the fact that the bulk appKTP crystal was designed for broad fundamental pulses ($\Delta\lambda \sim 7$ nm). However, the single-pass SHG scheme of Fig. 2 allows tight focusing of the fundamental beam in the center of a bulk SHG crystal in order to generate sufficiently high intensities for efficient nonlinear conversion. Although the aperiodic structure in the bulk appKTP crystal varied from 4.1 to 4.3 μm over a length of 4 mm, the associated confocal parameter (estimated to be the distance over which SHG takes place) is only 0.3 mm. Therefore, in the case of such tight focusing, the fundamental field will not experience the full gradient of the aperiodic structure. As such, the effective fundamental bandwidth is narrowed. The optimum 7-nm bandwidth indicated by Fig. 4(b) represents an expected expansion of the wavelength response due to the broadband fundamental.

D. Waveguide appKTP

The need for tight focusing in the bulk appKTP crystal (above) at relatively low power levels (~30 mW) resulted in some narrowing of the available phasematching bandwidth. This is easily avoided by using a waveguided structure, where the full aperiodicity of the appKTP structure can be utilized.

The waveguide appKTP crystal was fabricated using rubidium ion-exchange, with cross-sectional dimensions of ~4×4 μm and length of 12 mm. The waveguide, which was not AR-coated, was designed for single-mode transmission and for a fundamental bandwidth of 11 nm (i.e., for SHG of 839–851 nm). The linear grating chirp is represented by a change in grating period from 3.8 to 4.0 μm.

With a suitable coupling lens of 6.2-mm focal length, up to 5.4 mW of blue average power at around 422 nm was obtained from 24.8 mW of fundamental. The internal SHG efficiency reached a maximum of 32%, with an overall system electrical-to-blue efficiency of 0.4%.

The effects of utilizing the full aperiodicity of the appKTP waveguide structure was evident when observing the generated blue spectral bandwidths. Whereas the bulk appKTP crystal provided blue spectra with bandwidths of around 1 nm, broader blue spectra up to ~2.5 nm were observed [Fig. 5(b)], which supported shorter duration blue pulses. The structured oscillatory nature of the blue spectral profile, also recently observed elsewhere [26], is discussed in Section V-B.

Tunability of the blue light from 418 to 429 nm was also possible, via simple tuning of the Cr:LiSAF pump laser. This 11-nm tuning range coincides with the fundamental acceptance bandwidth of 11 nm for which the appKTP waveguide was designed.

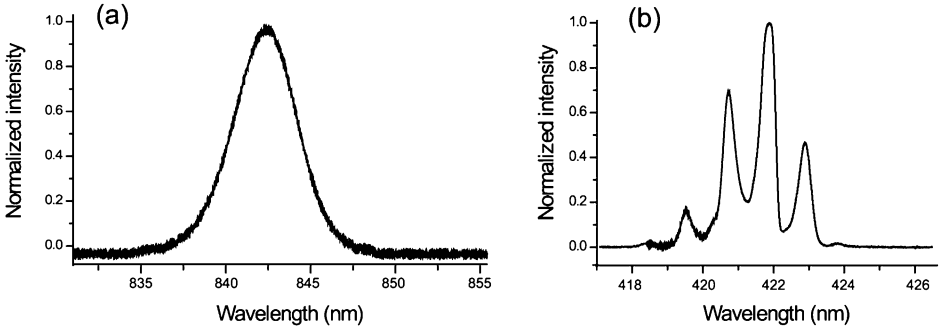

Fig. 5. (a) Spectrum of fundamental pulses transmitted through the waveguide appKTP crystal ($\Delta\lambda \sim 5$ nm). (b) Typical structured spectra of blue pulses leaving the waveguide, with an FWHM spectral bandwidth of up to approximately 2.5 nm.

V. Modeling of SHG Crystal Performance

A. Bulk SHG Crystals

The efficiency of any SHG process is subject to limitations imposed by group velocity mismatch (GVM), which describes a temporal walkoff between the interacting beams. At the risk of exaggerating the pulse-broadening effects of GVM, a "thick" $KNbO_3$ crystal was used above to obtain very high conversion efficiencies [11], [18], [19].

Elsewhere, we have reported a theoretical model that defines the optimal focusing conditions for SHG using focused beams in the ultrashort-pulse regime, in the conditions where GVM is significant. The model [27], verified by experiment [11], is suitable for cases when birefringence walkoff can be neglected, such as SHG with noncritical phasematching (as with $KNbO_3$) and SHG in a quasi-phasematched structure [28] (as with appKTP and ppKTP crystals). It provides information on the efficiency of the SHG process, the pulse duration of the SH pulses, and the modification of the phasematching tuning curves. It also allows for optimization of the SHG process by selecting the optimal phase mismatch, focusing strength, and position of focusing within the crystal.

As indicated in Section IV-A, a 15-mm focal-length lens was used to focus tightly into a "thick" crystal ($L = 3$ mm) of $KNbO_3$. It is useful to define this crystal length L in relation to the nonstationary length $L_{\rm nst}$, defined by $L_{\rm nst} = \tau/\alpha$, where τ is the time duration of the fundamental pulses and α is the GVM parameter. Typically, SHG crystals are chosen such that $L/L_{\rm nst} = 1$ in order to minimize the effects of GVM. (An SHG crystal is considered to be "thick" when $L/L_{\rm nst} > 1$.) The choice of focusing lens is also interesting because it provides optimization of the focusing strength, defined as $m = L/b$, where b is the confocal parameter, $b = {\rm k}w^2$, w is the focal spot radius, and k is the wave vector of the fundamental wave.

We have found, both experimentally and theoretically, that an optimum focusing strength m exists for a given SHG crystal length $L/L_{\rm nst}$ [27]. Therefore, for the SHG of ultrashort pulses, the optimal focusing strength $m_{\rm opt} = (L/b)_{\rm opt}$ for any given crystal length $L/L_{\rm nst}$ can be obtained from Fig. 6.

In our model, the normalized efficiency of the SHG process η_0 ($\%\ pJ^{-1}$) is calculated using the appropriate undepleted pump approximation [27]

$$\eta_0 = \frac{16\pi^2 d_{\rm eff}^2}{3\lambda^3 c\varepsilon_0 n_2 n_1}\frac{Lh_{\rm tr}}{\tau_{\rm SH}}10^{-10} \tag{1.1}$$

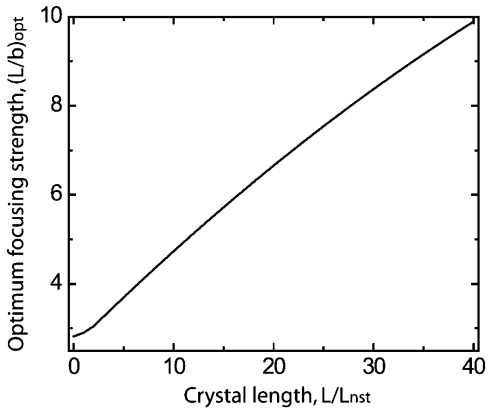

Fig. 6. Dependence of optimal focusing strength $m_{\rm opt} = (L/b)_{\rm opt}$ on crystal length $L/L_{\rm nst}$ [27]. Here, the efficiency of the SHG process using a bulk SHG crystal can be maximized by selecting the correct focusing lens for a given crystal length.

where n_2 and n_1 are, respectively, the refractive indexes at the SH and fundamental wavelengths, $\tau_{\rm SH}$ is defined as $\tau_{\rm SH} = \tau_0/1.76$, τ_0 is the FWHM fundamental pulse duration, and $h_{\rm tr}$ is a transient focusing factor [27]. Assuming that the pump depletion is weak, the absolute efficiency η (%) can also be calculated [29]

$$\eta = \frac{100W_{\rm fund}\eta_0}{100 + W_{\rm fund}\eta_0} \tag{1.2}$$

where $W_{\rm fund}$ is the fundamental pulse energy in picojoules. Fitting the experimental data from the $KNbO_3$ experiment with (1.2), we find an experimental value of $\eta_0 = 0.30\% pJ^{-1}$, whereas the theoretical value from (1.1) is $\eta_0 = 0.32\% pJ^{-1}$ (using $d_{\rm eff} = 12.5$ pmV^{-1}, $\tau_0 = 210$ fs, and, from the model in [27], a calculated value of $h_{\rm tr} = 0.137$). The agreement is illustrated in Fig. 7.

On this basis, we can now extend the approach given in [27] to describe the process of SHG with focused beams in aperiodically poled nonlinear media. To begin, let us first accept that a nonlinear crystal with a linearly chirped QPM grating can be described as a nonlinear medium with a locally varying phasematching parameter. As shown by Fejer and coworkers [25], [30], the phase factor which controls the SHG process is $\Phi(z) = \Delta k_0 z + D_g z^2$, which corresponds to $\Delta k(z) = d\Phi(z)/dz = \Delta k_0 + 2D_g z$, where D_g is calculated from $D_g = \pi\Delta\Lambda/(\Lambda_0^2 L)$ and $\Delta k_0 = k_2 - 2k_1 - 2\pi/\Lambda_0$. The terms $\Delta\Lambda$ and Λ_0 define the

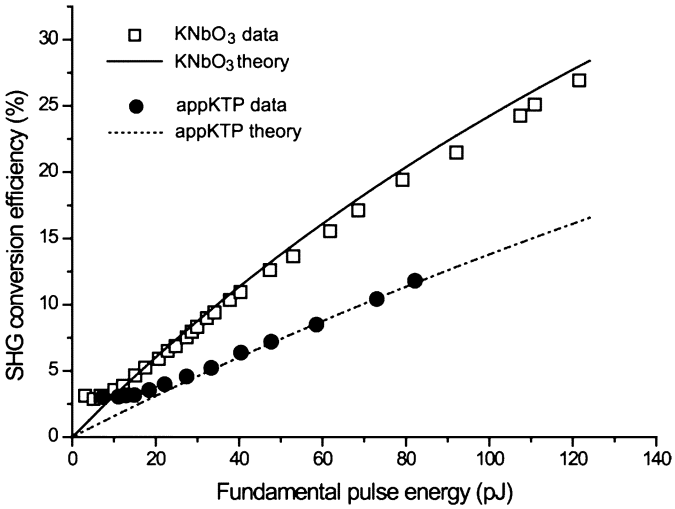

Fig. 7. Theoretical predictions versus experimental data for the performance of the bulk SHG crystals $KNbO_3$ and appKTP.

face-to-face grating period variation and the mean grating period, respectively. Note also that for sufficiently long samples, as is the case for both $KNbO_3$ and appKTP above, the variation of $\Delta\Lambda$ defines the wavelength acceptance bandwidth of the SHG process

$$\Delta\lambda_{\text{fund}} = \left| \frac{2\pi\Delta\Lambda}{\Lambda_0^2} \left(\frac{d\Delta k_0}{d\lambda} \right)^{-1} \right|. \tag{1.3}$$

(The calculated value for our waveguide appKTP crystal of $\Delta\lambda_{\text{fund}} = 12.6$ nm is in excellent agreement with the tests carried out on the sample after fabrication.)

To adapt the theory described in [27] for linearly chirped (aperiodically poled) QPM samples, it is necessary to replace the phase factor $\Phi(z) = \Delta k_0 z$ in formulas from [27] with the phase factor $\Phi(z) = (\Delta k_0 + D_g z)z$ and perform all the associated integrations. Meanwhile, (1.1) and (1.2) remain unchanged. Fitting the measured data for the bulk appKTP crystal to (1.2), we obtain the experimental value of $\eta_0 = 0.16\% pJ^{-1}$. From (1.1), we calculate the theoretical value of $\eta_0 = 0.16\% pJ^{-1}$ (using $d_{\text{eff}} = 7.8$ pmV^{-1}, $\tau_0 = 210$ fs and a calculated value of $h_{\text{tr}} = 0.087$). Once again, Fig. 7 illustrates the accuracy of the model to experimental observations.

It is worth repeating that the relatively low efficiency for the appKTP crystal is due to the fact that $d_{\text{eff}}(\text{KTP}) < d_{\text{eff}}(\text{KNbO}_3)$. Performing the same assessment with lithium niobate (LiNbO_3) should yield up to four times the efficiency, because $d_{\text{eff}}\ (\text{LiNbO})_3 = 17.6$ pmV^{-1}.

As mentioned earlier, insufficient power was available to measure the duration of the blue pulses from the bulk appKTP crystal. Calculation shows that the pulses, with an uncompensated duration of 370 fs, can be compressed to 270 fs in order to access higher peak powers.

We find also that the strong dependence of crystal length L/L_{nst}, on optimum focusing strength, $m_{\text{opt}} = (L/b)_{\text{opt}}$, exhibited by materials with constant Δk (Fig. 6) no longer applies when dealing with aperiodically poled structures (those with a linear change in Δk).

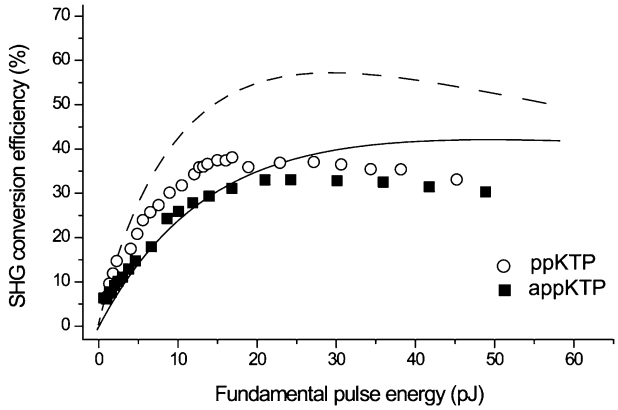

Fig. 8. Saturation of SHG efficiency in the waveguide (ppKTP and appKTP) experiments (point data). Theoretical predictions incorporating the effects of TPA for the SH wave and group velocity mismatch are also shown for the ppKTP (dashed line) and appKTP waveguides (solid line).

We believe that our model can be extended further to accurately describe other nonlinear optical interactions such as sum and difference frequency mixing, as well as higher order harmonic generation.

B. Waveguide SHG Crystals

When using the waveguide ppKTP crystal, the dependence of internal SHG efficiency on input power is characterized by a maximum efficiency of 37%. A further increase in fundamental pulse energy then leads to a saturation and subsequent decrease in the efficiency of the SHG process (Fig. 8). This behavior was also observed in the waveguide appKTP crystal (Fig. 8) and has been reported elsewhere [21], [26]. As we have suggested previously [12], two-photon absorption (TPA) of the SH wave is the most likely explanation for this behavior.

In Fig. 8, we provide theoretical curves for the performance of the waveguide crystals, which account for the observed effects of TPA. To achieve this, we solved differential (1.4), which account for the temporal behavior of the interacting pulses, the nonlinear losses of the SH wave, and the possible z dependence of the phasematching condition

$$\begin{aligned} \left(\frac{\partial}{\partial z} + \frac{1}{v_1}\frac{\partial}{\partial t} \right) A_1 &= -i\sigma_1 A_2 A_1^* \exp[-i\Phi(z)] \\ \left(\frac{\partial}{\partial z} + \frac{1}{v_2}\frac{\partial}{\partial t} \right) A_2 &= -i\sigma_2 A_1^2 \exp[i\Phi(z)] - \gamma A_2^2 A_2^* \end{aligned} \tag{1.4}$$

where A_1 and A_2 are the complex amplitudes of the fundamental and SH waves, respectively, and are functions of (z, t). The nonlinear coupling coefficients $\sigma_{1,2}$ are calculated as $\sigma_{1,2} = 2\pi d_{\text{eff,SHG}}/(\lambda n_{1,2})$, where the magnitude of $d_{\text{eff,SHG}}$ for QPM waveguides is $d_{\text{eff,SHG}} = (2/\pi)d_{33}\beta$, and β is an overlap integral and is < 1. The terms v_1 and v_2 represent the group velocities of the fundamental and SH waves, respectively, and are used to define the GVM parameter, as mentioned earlier, as $\alpha = 1/v_2 - 1/v_1$.The parameter $\gamma = (3\pi/4\lambda_2 n_2)\text{Im}(\chi^{(3)})$ where $\text{Im}(\chi^{(3)})$ is the imaginary part of the third-order nonlinear susceptibility [31]. The phase factor in system (1.4) is defined as $\Phi(z) = \Delta k_0 z$ for the ppKTP waveguide and $\Phi(z) = \Delta k_0 z + D_g z^2$ for the appKTP waveguide.

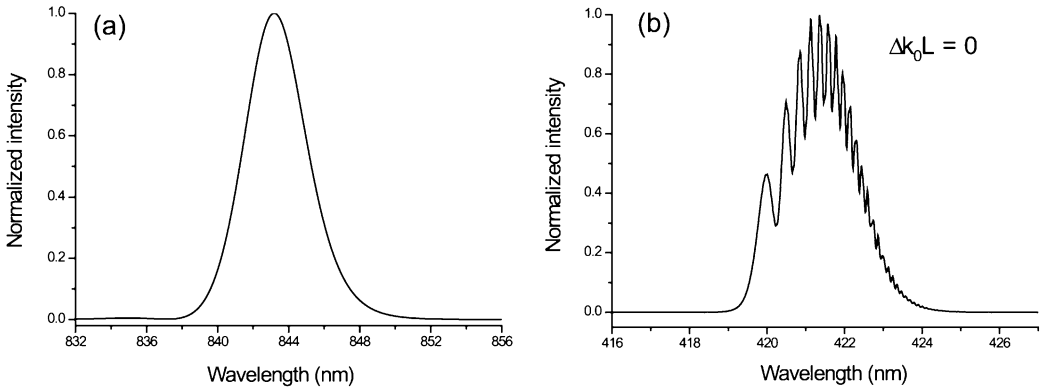

Fig. 9. Theoretically calculated output spectra for (a) the fundamental and (b) SH wave, at 50-pJ input pulse energy and $\Delta k_0 L = 0$. See Fig. 5 for experimental spectra.

The effect of TPA of the SH wave is to bring into imbalance the conservation of energy at the waveguide output. Experimental observations [12] have shown that, for input fundamental pulse energies of around 60 pJ, the ratio of $(P_{1,\mathrm{out}} + P_{2,\mathrm{out}})/P_{1,\mathrm{in}}$ reached 75%, where P_1 and P_2 are, respectively, the average powers of the fundamental and SH beams. As the exact value of $\mathrm{Im}(\chi^{(3)})$ for KTP at 430 nm is, to our knowledge, not available in the literature; we have used these measured nonlinear-type losses in energy to adjust the value of the parameter γ in the system (1.4).

The theoretical curves obtained from the solution of system (1.4), with $\gamma = 0.03L\sigma^2$, are shown in Fig. 8. If we take $d_{\mathrm{eff,SHG}} = 3.6$ pm/V, the value of γ used in the calculation corresponds to a TPA coefficient of 3.8 cm/GW, which is close to the reported TPA coefficient of $KNbO_3$ (3.2 cm/GW) [32].

The horizontal scales are normalized to match the initial slopes of the experimental curves. It is clear that the presence of TPA causes the slight decrease in SHG efficiency once saturation of the SHG process has begun. The fact that the measured efficiency is less than that predicted by the theory shows that the model can be improved further. This could be achieved by accounting for other effects such as nonlinear losses of the SH wave due to presence of the fundamental wave, self-phase and cross-phase modulation, and blue-light induced red absorption (BLIRA) [32], [33]. Thermally induced phase mismatch may also be present as the blue wavelength is close to the absorption edge of the crystal.

In addition, theoretical output spectra for the fundamental and SH waves for the appKTP waveguide are shown in Fig. 9. It can be seen that they closely represent the observed experimental oscillatory nature of the SH spectra and the smooth profile of the fundamental output, as shown in Fig. 5. Our calculations predict that the oscillations in Fig. 9(b) become more exaggerated as we tune away from the perfect phasematching condition.

VI. Discussion and Summary

Of the four SHG crystals investigated in this paper (Fig. 10), bulk $KNbO_3$, was superior both in terms of generated blue average power (11.8 mW) and overall electrical-to-optical efficiency (1%). $KNbO_3$ is also less susceptible to the observed saturation and subsequent decrease in SHG efficiency observed in both waveguide crystals.

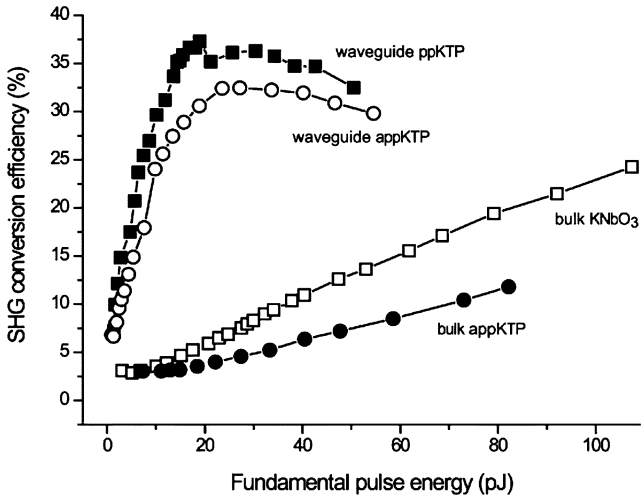

Fig. 10. Relative performance of the four SHG crystals investigated in this paper as a means to efficiently and practically generate ultrafast blue light from a compact and portable femtosecond Cr:LiSAF laser.

The appKTP waveguide provided similar maximum internal SHG efficiency (32%) to that of a ppKTP waveguide (37%), and the steep rise in SHG efficiency proves the effectiveness of such waveguides under low pump-pulse-energy conditions. In addition, the broad wavelength acceptance bandwidth of the appKTP waveguide enabled the blue pulses to be tuned from 418 to 429 nm by frequency tuning of the Cr:LiSAF laser.

Blue spectral widths of up to ~2.5 nm and corresponding theoretical analyses confirm that significantly shorter blue pulse durations are obtained when aperiodic poling rather than periodic poling is used. As a result, higher peak power blue pulses can be generated with the bulk and waveguide appKTP crystals. Bulk appKTP is not ideally suited to low-power sources that require tight focusing to access sufficiently high intensities, although another advantage is the absence of efficiency saturation. Conveniently, all four crystals perform well at room temperature such that minimal wavelength and temperature stabilizations are required.

The theoretical model of SHG with focused beams in both homogeneous and linearly chirped aperiodically poled structures predicts very well the results from the bulk $KNbO_3$ and bulk appKTP crystals. The model of SHG in the two waveguide

TABLE I

SUMMARY OF THE PERFORMANCE OF THE FOUR SHG CRYSTALS L:SHG CRYSTAL LENGTH (cm); α: GVM PARAMETER (ps.mm^{-1}); b: CONFOCAL PARAMETER (mm) ; f: FOCAL LENGTH (mm); $P_{\rm SH}$: BLUE AVERAGE POWER (mW); η_{SHG}: MAXIMUM SHG CONVERSION EFFICIENCY (%); $\eta_{\rm slope}$: SHG SLOPE EFFICIENCY PER UNIT CRYSTAL LENGTH (% pJ^{-1} cm^{-1}); $\eta_{\rm elec}$: ELECTRICAL-TO-BLUE SYSTEM EFFICIENCY (%); $Ep_{\rm SH}$: BLUE PULSE ENERGY (pJ); $\Delta\lambda_{\rm SH}$: BLUE SPECTRAL BANDWIDTH (nm)

	bulk KNbO3	waveguide ppKTP	bulk appKTP	waveguide appKTP
L	0.3	0.8	0.4	1.2
α	1.2	1.2	1.2	1.2
b	0.31	-	0.25	-
f	15	-	15	-
P_{SH}	11.8	5.6	3.2	5.4
η_{SHG}	30	37	12	32
η_{slope}	1	6.9	0.4	2.3
η_{elec}	1	0.5	0.3	0.4
Ep_{SH}	36	17	10	16
$\Delta\lambda_{SH}$	<1.4	0.6	<1.4	~2.5

crystals explains qualitatively the saturation and subsequent decrease of the SHG efficiency, but requires further refinement to explain more fully the experimentally observed absolute efficiency.

In choosing the right SHG crystal for use in the portable ultrafast blue light source described in this paper, the advantages of using bulk, waveguide, periodically poled or aperiodically poled media can be exploited with the intended application in mind. The relative performance of the four SHG crystals is summarized in Table I.

VII. CONCLUSION

We have described an effective means of achieving a practical, robust, and portable ultrafast blue light source using a compact femtosecond Cr:LiSAF laser in conjunction with selected frequency-doubling crystals. All configurations made use of a very simple extracavity, single-pass arrangement for optimal and efficient SHG at room temperature, requiring minimal stabilization. Our expectation is that such a compact laser design will be of increasing interest to researchers and technologists engaged in photonics-based system developments and applications.

REFERENCES

[1] P. N. Prasad, "Bioimaging: Principles and techniques," in *Introduction to Biophotonics*. New York: Wiley, 2003, pp. 203–254.

[2] H. Schnitzler *et al.*, *Appl. Opt.*, vol. 41, no. 33, pp. 7000–7005, 2002.

[3] R. S. Knox, "Ultrashort processes and biology," *J. Photochem. Photobiol.*, vol. 49, pp. 81–88, 1999.

[4] W. Rudolph, P. Dorn, X. Liu, N. Vretenar, and R. Stock, "Microscopy with femtosecond laser pulses: Applications in engineering, physics and biomedicine," *Appl. Surface Sci.*, vol. 208, pp. 327–332, 2003.

[5] S. W. Hell *et al.*, "Pulsed and cw confocal microscopy—A comparison of resolution and contrast," *Opt. Commun.*, vol. 113, no. 1–3, pp. 144–152, 1994.

[6] B. Agate, C. T. A. Brown, W. Sibbett, and K. Dholakia, "Femtosecond optical tweezers for *in situ* control of two-photon fluorescence," *Opt. Expr.*, vol. 12, no. 13, pp. 3011–3017, 2004.

[7] P. J. Campagnola, M. D. Wei, A. Lewis, and L. M. Loew, "High-resolution nonlinear optical imaging of live cells by second harmonic generation," *Biophys. J.*, vol. 77, no. 6, pp. 3341–3349, 1999.

[8] E. Bordenave, E. Abraham, G. Jonusauskas, J. Oberle, and C. Rulliere, "Longitudinal imaging in biological tissues with a single laser shot correlation system," *Opt. Expr.*, vol. 10, no. 1, pp. 35–40, 2002.

[9] L. Zhu, P. Li, J. T. Sage, and P. M. Champion, "Femtosecond dynamics of heme-proteins," *J. Luminescence*, vol. 60, no. 1, pp. 503–506, 1994.

[10] B. Agate, B. Stormont, A. J. Kemp, C. T. A. Brown, U. Keller, and W. Sibbett, "Simplified cavity designs for efficient and compact femtosecond Cr:LiSAF lasers," *Opt. Commun.*, vol. 205, pp. 207–213, 2002.

[11] B. Agate, A. J. Kemp, C. T. A. Brown, and W. Sibbett, "Efficient, high repetition-rate femtosecond blue source using a compact Cr:LiSAF laser," *Opt. Expr.*, vol. 10, no. 16, pp. 824–831, 2002.

[12] B. Agate, E. U. Rafailov, W. Sibbett, S. M. Saltiel, P. Battle, T. Fry, and E. Noonan, "Highly efficient blue-light generation from a compact, diode-pumped femtosecond laser by use of a periodically poled KTP waveguide crystal," *Opt. Lett.*, vol. 28, no. 20, pp. 1963–1965, 2003.

[13] J.-M. Hopkins, G. J. Valentine, B. Agate, A. J. Kemp, U. Keller, and W. Sibbett, "Highly compact and efficient femtosecond lasers," *IEEE J. Quantum Electron.*, vol. 38, pp. 360–368, 2002.

[14] J.-M. Hopkins *et al.*, "Efficient, low-noise, SESAM-based femtosecond Cr^{3+} : $LiSrAlF_6$ laser," *Opt. Commun.*, vol. 154, no. 1–3, pp. 54–58, 1998.

[15] W. Sibbett *et al.*, "Compact femtosecond oscillators," in *Ultrafast Optics IV*, F. Krausz *et al.*, Ed., 2004.

[16] G. J. Valentine *et al.*, "Ultralow-pump-threshold, femtosecond Cr^{3+} : $LiSrAlF_6$ laser pumped by a single narrow-stripe AlGaInP laser diode," *Opt. Lett.*, vol. 22, no. 21, pp. 1639–1641, 1997.

[17] A. A. Lagatsky, E. U. Rafailov, C. G. Leburn, C. T. A. Brown, N. Xiang, O. G. Okhotnikov, and W. Sibbett, "Highly efficient femtosecond Yb:KYW laser pumped by a single narrow-stripe laser diode," *Electron. Lett.*, vol. 39, no. 15, pp. 1108–1110, 2003.

[18] A. M. Weiner, A. M. Kan'an, and D. E. Leaird, "High-efficiency blue generation by frequency doubling of femtosecond pulses in a thick nonlinear crystal," *Opt. Lett.*, vol. 23, no. 18, pp. 1441–1443, 1998.

[19] D. Gunzun, Y. Li, and M. Xiao, "Blue light generation in single-pass frequency doubling of femtosecond pulses in $KNbO_3$," *Opt. Commun.*, vol. 180, pp. 367–371, 2000.

[20] E. U. Rafailov, D. J. L. Birkin, W. Sibbett, P. Battle, T. Fry, and D. Mohatt, "Efficient direct frequency conversion of a nonresonant injection-seeded laser diode using a periodically-poled KTP waveguide crystal," *Opt. Lett.*, vol. 26, no. 24, pp. 1961–1962, 2001.

[21] Y. S. Wang, V. Petrov, Y. J. Ding, Y. Zheng, J. B. Khurgin, and W. P. Risk, "Ultrafast generation of blue light by efficient second-harmonic generation in periodically-poled bulk and waveguide potassium titanyl phosphate," *Appl. Phys. Lett.*, vol. 73, no. 7, pp. 873–875, 1998.

[22] D. J. L. Birkin *et al.*, "3.6 mW blue light by direct frequency-doubling of a diode laser using an aperiodically-poled lithium niobate crystal," *Appl. Phys. Lett.*, vol. 78, no. 21, pp. 3172–3174, 2001.

[23] D. Artigas and D. T. Reid, "Efficient femtosecond optical parametric oscillators based on aperiodically poled nonlinear crystals," *Opt. Lett.*, vol. 27, no. 10, pp. 851–853, 2002.

[24] P. Loza-Alvarez *et al.*, "Simultaneous femtosecond-pulse compression and second-harmonic generation in aperiodically poled $KTiOPO_4$," *Opt. Lett.*, vol. 24, no. 15, pp. 1071–1073, 1999.

[25] M. A. Arbore, O. Marco, and M. M. Fejer, "Pulse compression during second-harmonic generation in aperiodic quasiphase-matching gratings," *Opt. Lett.*, vol. 22, no. 12, pp. 865–867, 1997.

[26] I. A. Begishev *et al.*, "Limitation of second-harmonic generation of femtosecond Ti:Sapphire laser pulses," *J. Optical Soc. Amer. B*, vol. 21, no. 2, pp. 318–322, 2004.
[27] S. M. Saltiel, K. Koynov, B. Agate, and W. Sibbett, "Second-harmonic generation with focused beams under conditions of large group-velocity mismatch," *J. Optical Soc. Amer. B*, vol. 21, no. 3, pp. 591–598, 2004.
[28] M. M. Fejer, G. A. Magel, D. H. Jundt, and R. L. Byer, "Quasiphase-matched 2nd harmonic generation—Tuning and tolerances," *IEEE J. Quantum Electron.*, vol. 28, pp. 2631–2654, 1992.
[29] H. Wang and A. M. Weiner, "Efficiency of short-pulse type-I second-harmonic generation with simultaneous spatial walk-off, temporal walk-off, and pump depletion," *IEEE J. Quantum Electron.*, vol. 39, pp. 1600–1618, 2003.
[30] G. Imeshev, M. A. Arrbore, M. M. Fejer, A. Galvanauskas, and M. E. Fermann, "Ultrashort-pulse second-harmonic generation with longitudinally nonuniform quasiphase-matching gratings: Pulse compression and shaping," *J. Optical Soc. Amer. B*, vol. 17, no. 2, pp. 304–318, 2000.
[31] R. DeSalvo, M. Sheik-Bahae, A. A. Said, D. J. Hagan, and E. W. Van Stryland, "Z-scan measurements of the anisotropy of nonlinear refraction and absorption in crystals," *Opt. Lett.*, vol. 18, no. 3, pp. 194–194, 1993.
[32] A. D. Ludlow, H. M. Nelson, and S. D. Bergeson, "Two-photon absorption in potassium niobate," *J. Optical Soc. Amer. B*, vol. 18, no. 12, pp. 1813–1820, 2001.
[33] L. E. Busse, L. Goldberg, M. R. Surette, and G. Mizell, "Absorption losses in MgO-doped and undoped potassium niobate," *J. Appl. Phys.*, vol. 75, pp. 1102–1110, 1993.

Ben Agate received the M.Sci. and Ph.D. degrees in physics from the University of St. Andrews, St. Andrews, U.K., in 1998 and 2003, respectively.

He is presently working as a Research Fellow with the Interdisciplinary Centre for Medical Photonics, University of St. Andrews. His current research interests include the application of femtosecond laser systems in the field of biomedicine. He is coauthor of 23 journal and conference papers

Dr. Agate is an Associate Member of the U.K. Institute of Physics.

Edik U. Rafailov (M'01) received the M.Sc. degree (with honors) in physics from the Samarkand State University, Samarkand, U.S.S.R., and the Ph.D. degree in physics of semiconductors and dielectrics at A. F. Ioffe Institute, St. Petersburg, Russia, in 1986 and 1991, respectively.

He remained as a Senior Researcher at the Institute until 1997 when he moved to the University of St. Andrews, St. Andrews, U.K., as a Research Fellow. His main research interests include novel high-power continuous-wave short ultrashort-pulse and high-frequency laser diodes, nanostructures (quantum-dots), integrated and nonlinear optics, compact diode-based visible/IR/MIR lasers, and laser diode applications. He has coauthored over 95 journal and conference papers on these topics.

Wilson Sibbett received the B.Sc. degree in physics and Ph.D. degree in laser physics from the Queen's University, Belfast, U.K.

He joined the Blackett Laboratory, Imperial College, London, U.K., where he subsequently became a Lecturer and Reader in physics. In 1985, he moved to the University of St. Andrews, St. Andrews, U.K., as a Professor of natural philosophy and Head of the Department of Physics and where, since 1994, he has been the Director of Research. His main research interests include ultrashort-pulse lasers, diode lasers and diode-pumped solid-state lasers, nonlinear/waveguide optics and applications in photomedicine. He has coauthored over 300 journal publications on these topics.

Prof. Sibbett is a Fellow of the Royal Society (London), a Fellow of the Royal Society of Edinburgh, and has Fellowships from the Institute of Physics and the Optical Society of America.

Solomon M. Saltiel was born in Sofia, Bulgaria, in 1947. He received the M.S. and Ph.D. degrees from Moscow State University, Moscow, U.S.S.R., in the field of nonlinear optics in 1973 and 1976, respectively.

In 1976, he joined the Faculty of Physics, Sofia University, as an Associate Professor. In 1995 he received the position of Professor. He was with the University of California, Irvine, in 1988 and 1989. He has worked on collaborations with LPL, University Paris-13, the Nonlinear Physics Group, Australian National University, LOA- Ecole Politechnique, France, and the School of Physics and Astronomy, University of St. Andrews, U.K. His research interests include nonlinear optics and laser spectroscopy. He has published two book chapters and is coauthor of over 100 journal articles and three student textbooks.

Prof. Saltiel is a member of Optical Society of America and Union of Physicists in Bulgaria.

Kaloian Koynov received the Ph.D. degree from Sofia University, Sofia, Bulgaria, in 1997.

He is presently working as a Researcher at Max Planck Institute for Polymer Research, Mainz, Germany. His current research interests include optoelectronic properties of thin polymer films and nonlinear optics.

Mikael Tiihonen, photograph and biography not available at the time of publication.

Shunhua Wang, photograph and biography not available at the time of publication.

Fredrik Laurell, photograph and biography not available at the time of publication.

Philip Battle, photograph and biography not available at the time of publication.

Tim Fry, photograph and biography not available at the time of publication.

Tony Roberts, photograph and biography not available at the time of publication.

Elizabeth Noonan, photograph and biography not available at the time of publication.